Supporting Information for

# Single-Molecule Visualization of DNase I-Mediated DNA Cleavage by High-Speed Atomic Force Microscopy

Nada Elessawy[1], Selma Sinan[2], Hongshan Zhang[2], Zhenglin Yang[1], Yi Lu[1], Ilya J. Finkelstein[2], and Yi-Chih Lin[1,*]

[1]Department of Chemistry, University of Texas at Austin, Austin, TX 78712, United States
[2] Department of Molecular Biosciences and Institute for Cellular and Molecular Biology, University of Texas at Austin, Austin, TX 78712, United States

*Correspondence to: Yi-Chih Lin (yichih.lin@utexas.edu)



**This PDF includes:**

## Materials and Methods

### Protein and DNA samples

DNase I (EN0521; Thermo Fisher Scientific) was used directly for HS-AFM experiments without further purification. The first 800 bp linear dsDNA substrate was generated directly by PCR amplification of the HPV-16 plasmid (45113; ATCC) using primers flanking the target region; no restriction enzyme digestion was required for linearization. The PCR product was run on an agarose gel, and the 800 bp band was purified using the Gel and PCR Clean-up System (A9281; Promega), followed by elution in nuclease-free water. A second linear 800 bp dsDNA substrate containing a CTCF binding site was prepared by PCR amplification of a synthesized dsDNA fragment (IDT).[1] Circular ss-DNA plasmid (N4040S, M13mp18; New England Biolabs) was used directly for HS-AFM experiments without further purification. Circular dsDNA plasmid was purified from the CMV-based mammalian expression vector pEGFP-N1 (Clontech) using standard plasmid purification procedures.[2] Plasmid DNA was then prepared from E. coli cultures using a column–based miniprep kit (QIAGEN) following the manufacturer's instructions and eluted in TE buffer.

### HS-AFM experiments

All HS-AFM movies were acquired using amplitude-modulation mode on a HS-AFM system (RIBM, Japan). Imaging conditions were performed in buffer solutions summarized in **Table S2**. Ultrashort Cantilevers (NanoWorld) with a spring constant of ~0.15 N/m, resonance frequency of ~600 kHz, and a quality factor of ~1.5 in buffer solutions were used for all HS-AFM experiments. The mica substrate was pretreated with 0.05% (v/v) APTES in water for 3 min, rinsed thoroughly with Milli-Q water, and used immediately for sample deposition prior to imaging.

*Single molecule characterization of DNase I.* DNase I was diluted to a concentration of 34 nM in imaging buffer and deposited on APTES-pretreated mica for 5 min prior to HS-AFM imaging.

*Realtime visualization of DNase I activity.* Linear dsDNA sample (1μL of 1 nM) was deposited on APTES-pretreated mica for 1-3 min. DNase I was then added to the mica substrate to a final concentration of 0.34–3.4 nM and incubated for 30 s to 2 min before HS-AFM imaging.

*Live addition of DNase I.* Linear dsDNA sample (1μL of 1 nM) was deposited on APTES-pretreated mica for 5 min before HS-AFM experiments. DNase I was subsequently introduced into the liquid cell at 90 s & 878 s after the start of image acquisition, reaching a final concentration of ~0.38 nM.

*DNase I-mediated DNA degradation experiments.* DNase I was first diluted to a concentration of 3.4 nM in buffer containing either EDTA, $Ca^{2+}$ alone, $Mg^{2+}$ alone, or both $Ca^{2+}$ and $Mg^{2+}$, and incubated for 30 min prior to mixing with DNA substrates. DNA substrates, including synthetic linear 800 bp dsDNA, circular ss-DNA plasmid, or circular dsDNA plasmid, was preincubated with DNase I under specific biochemical conditions for 30 min before HS-AFM imaging.

### Image processing and data analysis

All HS-AFM movies were processed using polynomial background removals built-in in ImageJ. Some movies were further processed with median filter (1 pixel in radius) to remove scanning noise. Volumes of DNase I particles were quantified in ImageJ by applying a height threshold to generate binary masks of individual particles, followed by volume estimation. Normalized cross correlation (NCC) score was calculated using the template matching plugin in ImageJ.[3] Prior to analysis, particles of interest were aligned to the center by translational registration, and NCC values were computed by comparing each frame to the initial reference frame. Kymograph of linear dsDNA cleavage by monomeric DNase I were generated by re-slicing HS-AFM image stacks along the DNA contour and applying a maximum-intensity z-projection to visualize protein position and DNA length changes over time.

**References:**

(1) Zhang, H.; Shi, Z.; Banigan, E. J.; Kim, Y.; Yu, H.; Bai, X.-c.; Finkelstein, I. J. CTCF and R-loops are boundaries of cohesin-mediated DNA looping. *Molecular Cell* **2023**, *83* (16), 2856–2871.e2858. DOI: 10.1016/j.molcel.2023.07.006

(2) Xiong, M.; Yang, Z.; Lake, R. J.; Li, J.; Hong, S.; Fan, H.; Zhang, X. B.; Lu, Y. DNAzyme-Mediated Genetically Encoded Sensors for Ratiometric Imaging of Metal Ions in Living Cells. *Angew Chem Int Ed Engl* **2020**, *59* (5), 1891–1896. DOI: 10.1002/anie.201912514

(3) Thomas, L. S. V.; Gehrig, J. Multi-template matching: a versatile tool for object-localization in microscopy images.

## Supplementary Figures

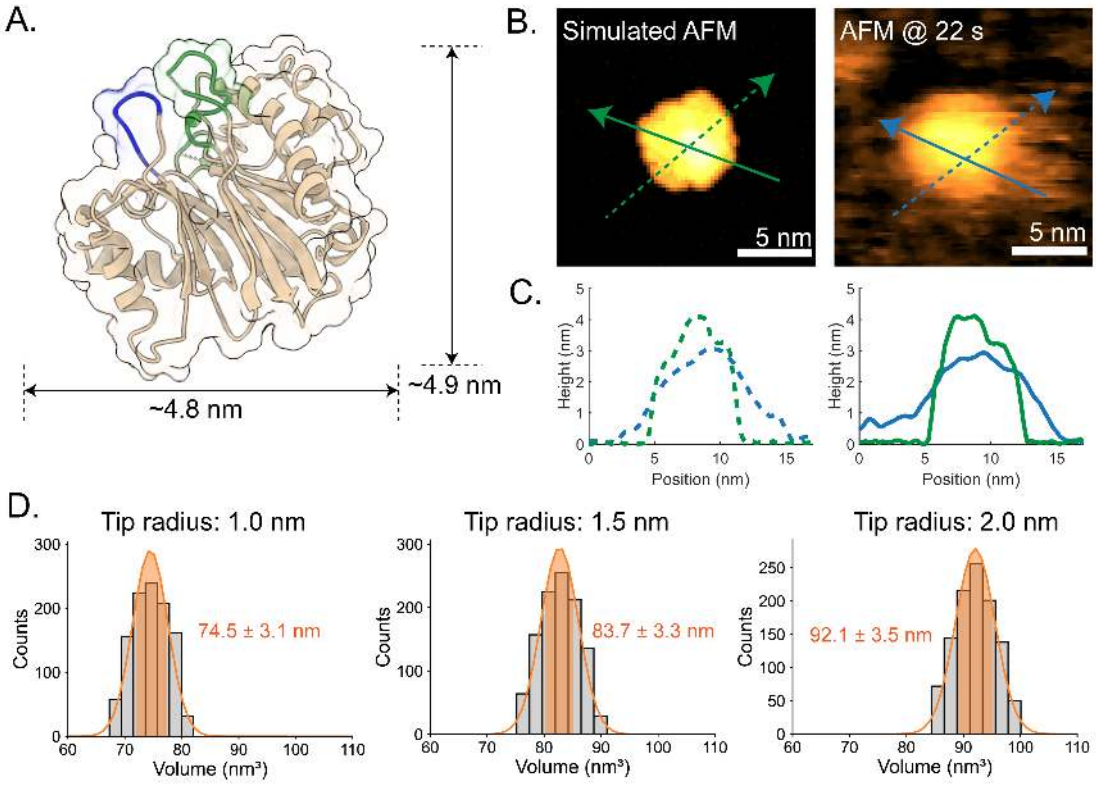


**Figure S1. Structural analysis of DNase I monomer. (A)** Structure of DNase I monomer (PDB: 3dni). For comparison with the HS-AFM data, the original PDB structure was rotated by 50°, 90°, and 95° about the x-, y-, z-axis, respectively. **(B)** Simulated AFM (left) and experimental HS-AFM images (right) of DNase I monomer. Briefly, the simulated AFM image was created by using a computational, user-defined tip geometry (1.0 nm radius at tip apex with a 15° sidewall angle) to convolute the surface topology of PDB structure, as shown in **(A)**. The orientation of the PDB structure is optimized based on the simulated AFM output with the best fit to experimental data in dimensions, which is the highest cross-correlation score. **(C)** The height cross-sectional profiles between the simulated (dashed lines) and experimental HS-AFM data (solid lines) highlight the similarity of molecular topologies. **(D)** Volume distributions of DNase I in simulated AFM images when the protein is rotated by 1° increments in the x-, y-axis, and xy-plane and probed with tip radii at 1.0, 1.5, and 2.0 nm, respectively.

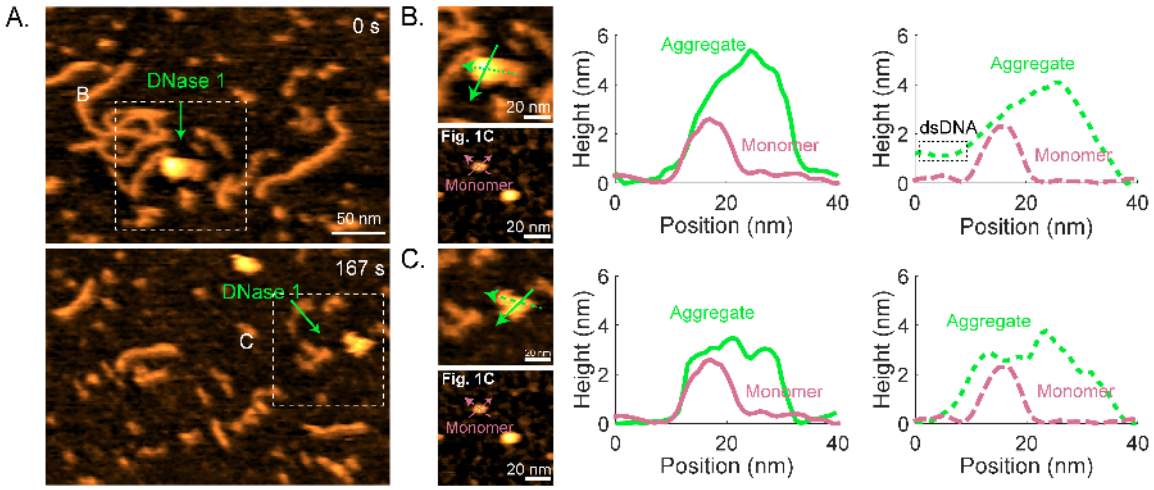


**Figure S2. Structural characterization of functional DNase I aggregates. Extended data for Figure 2A-D. (A)** Region of interest where two DNase I aggregate digests dsDNA. **(B-C)** Cross-sectional height profiles of the functional DNase I aggregates shown in **(A)** compared with the DNase I monomer reference from **Figure 1C.** The measured lateral dimensions and apparent heights of both aggregates match the expected dimensions of DNase I trimers, supporting their assignment as functional trimeric aggregates.

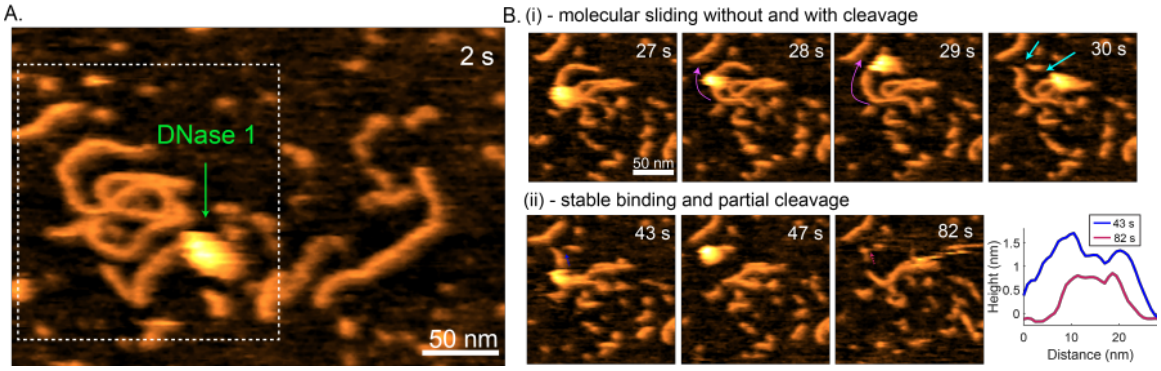


**Figure S3. Aggregated DNase I cleavage activity on linear dsDNA. Extended data for Figure 2A-2B. (A)** Region of interest where DNase I aggregate digests dsDNA. **(B)** Highlighted interactions and cleavage of linear dsDNA, including (i) sliding with and without cleavage and (ii) ss-breaks along the dsDNA.

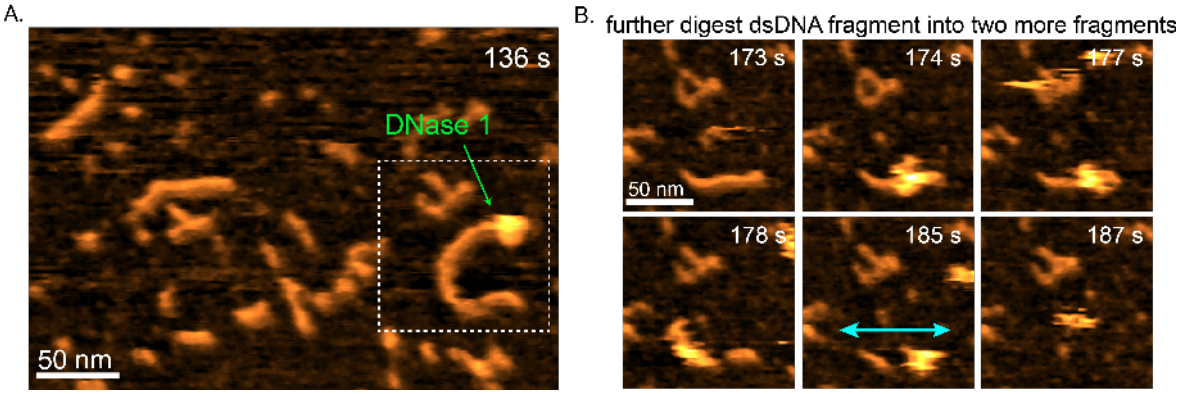


**Figure S4. Aggregated DNase I cleavage activity on linear dsDNA. Extended data for Figure 2D. (A)** Region of interest where DNase I aggregate digests dsDNA. (**B**) Highlighted interactions and cleavage of linear dsDNA where the DNase I aggregate breaks a fragment of dsDNA into two fragments, then separately interrogates each fragment until complete digestion.

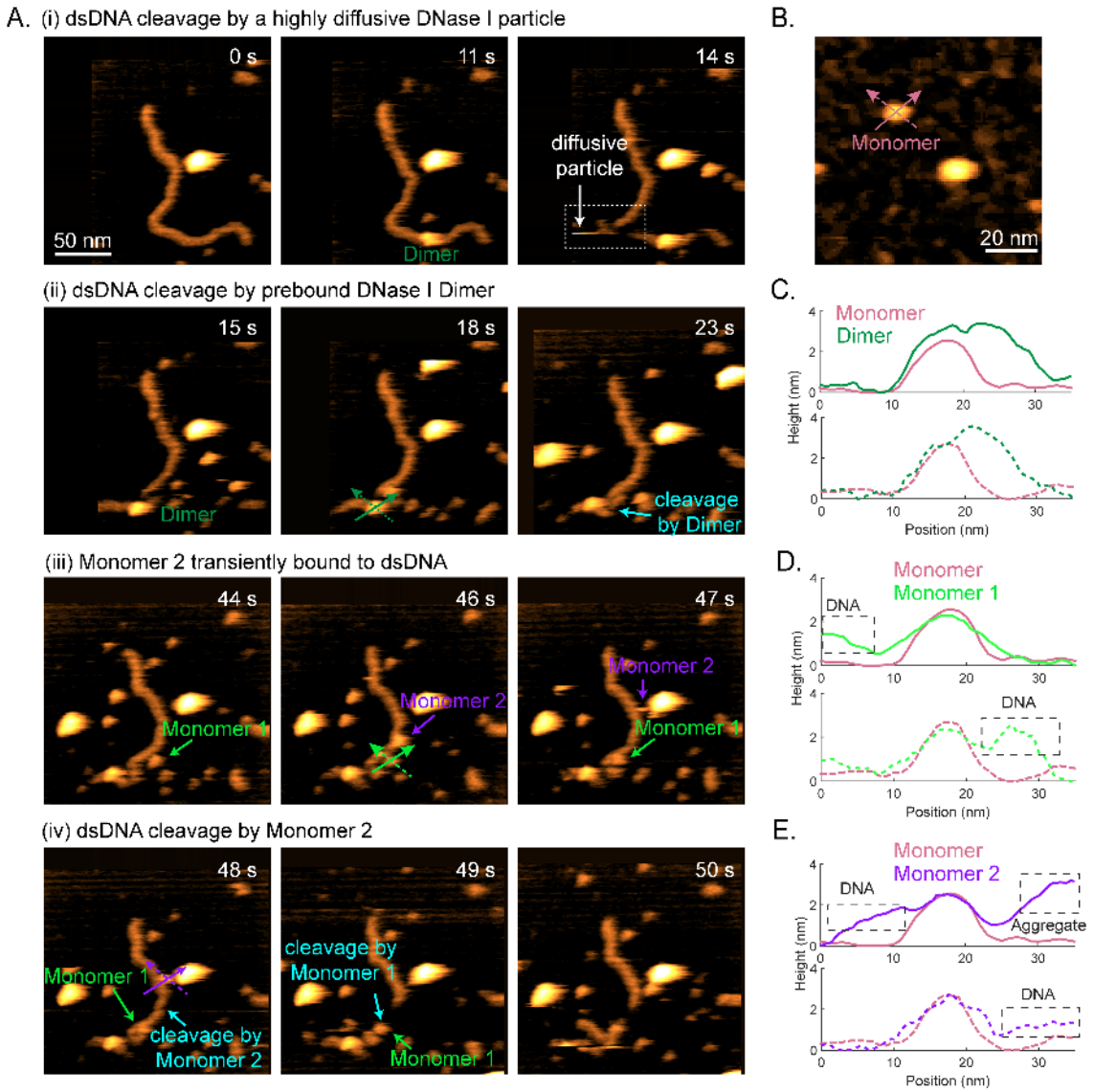


**Figure S5. Real-time HS-AFM observations of DNase I monomer and dimer cleavage activity on a linear 800 bp dsDNA substrate. (A)** Representative HS-AFM images showing dsDNA cleavage by (i) a highly diffusive DNase I particle, (ii) a DNase I dimer, and (iii-iv) two distinct DNase I monomers. **(B)** Representative HS-AFM image of a DNase I monomer from **Figure 1C**. **(C-E)** Cross-sectional height profile comparisons **(C)** between the DNase I monomer shown in **(B)** and a DNase I Dimer in **(A-ii**, 18 s**)**, **(D)** Monomer 1 in **(A-iii**, 46 s**)**, and **(E)** monomer 2 in **(A-iv**, 48 s**).** We first observed a DSB by a highly diffusive DNase I particle (**Figure S5A-i**, 14s) followed by a DSB of a stably bound DNase I dimer (**Figure S5A-ii**, 23s). Lastly, two monomers were observed cleaving the dsDNA fragment, with monomer 2 bound ~ 1 second to the fragment (**Figure S5A-iii-iv**).

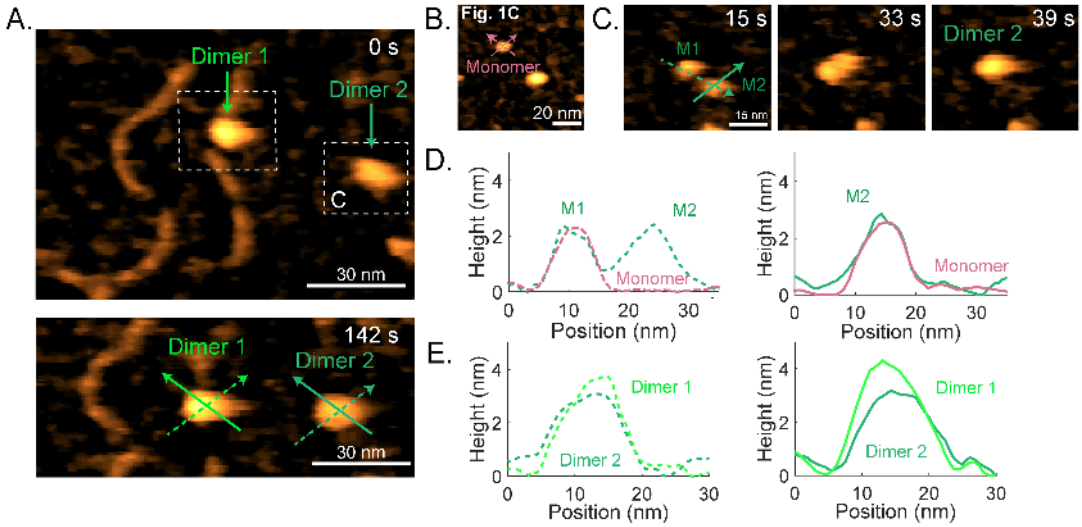


**Figure S6. Cleavage activity of a DNase I dimer on linear ds-DNA. Extended data for Figure 2E. (A)** Representative HS-AFM image showing two DNase I dimers. Dimer 1 cleaves dsDNA and is also observed on mica at 142 s. **(B)** Representative HS-AFM image of a DNase I monomer from **Figure 1C**. **(C)** Dissociation and reassociation dynamics of DNase I Dimer 2. **(D)** Cross-sectional height profiles of the dissociated monomers, M1 and M2 from Dimer 2. **(E)** Cross-sectional height-profile comparison of Dimer 1 and Dimer 2. Functionally active Dimer 1 exhibits a height consistent with the combined contribution of DNase I dimer and the underlying dsDNA substrate, which contributes ~1.2 nm in height, whereas Dimer 2 is measured on mica without DNA bound.

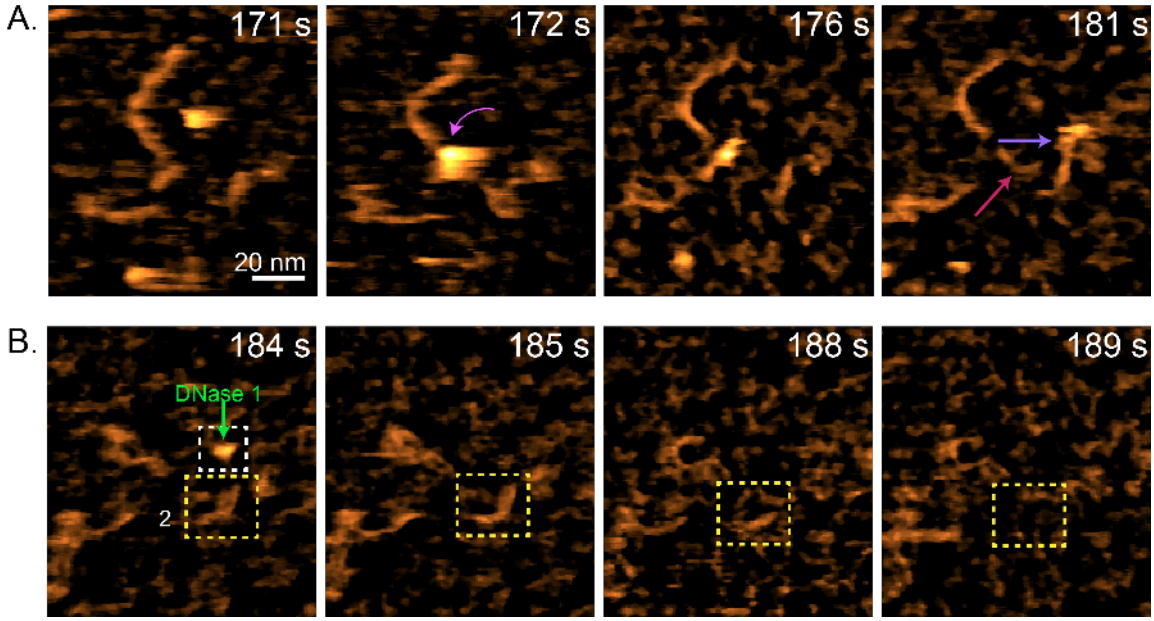


**Figure S7. Dimeric DNase I cleavage activity on linear dsDNA. Extended data for Figure 2E. (A)** DNase I dimer diffuses to and partially cleaves another dsDNA fragment after the full digestion of fragment 1 (F1 in **Figure 2E**). **(B)** Although DNase I dimer is not visible after 185 s, fragment 2 (F2 in **Figure 2E**) continues degradation from 185 s to189 s.

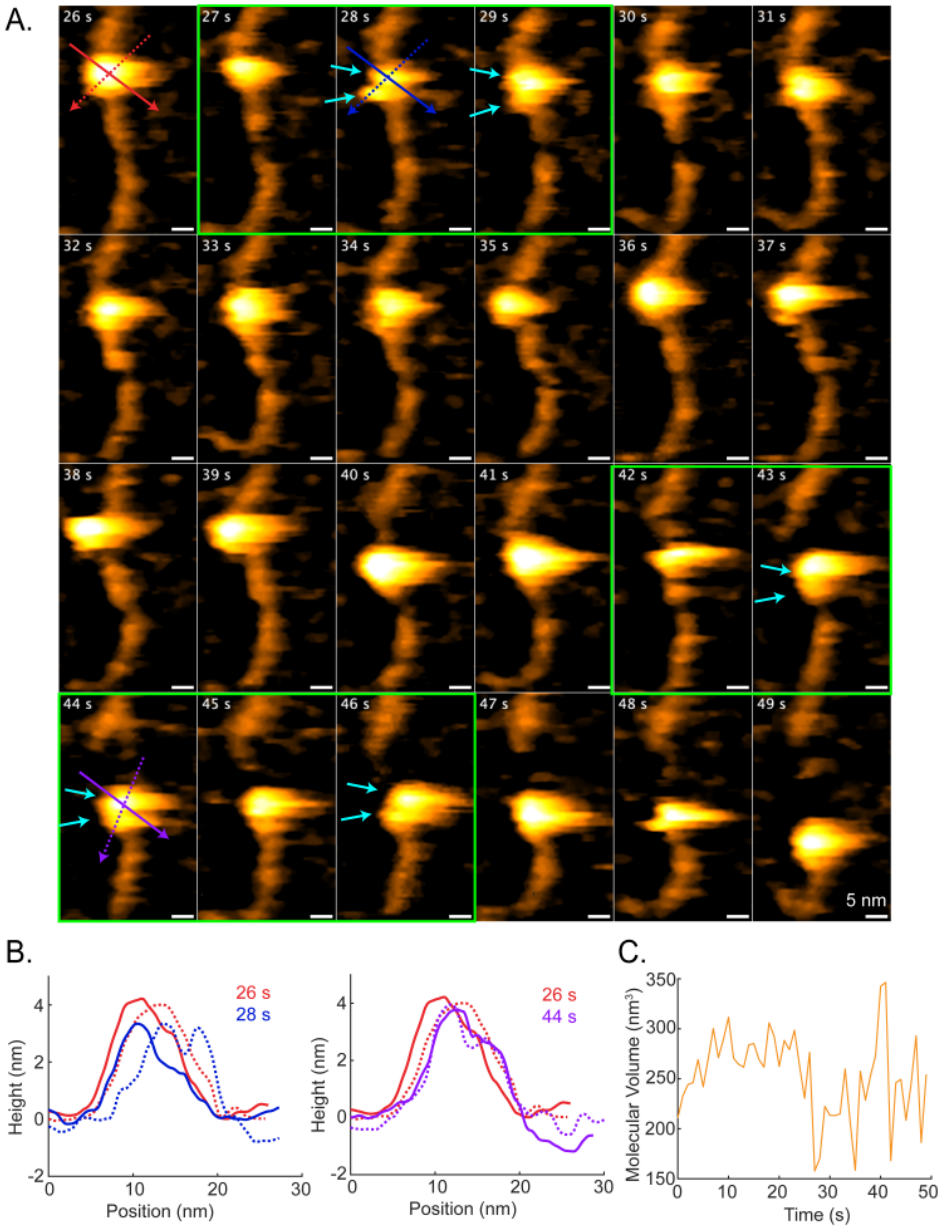


**Figure S8. Analysis of the two-lobed morphology of a DNase I dimer during dsDNA cleavage. Extended data for Figure 2E. (A)** Zoom-in HS-AFM images showing a DNase I dimer cleaving a dsDNA fragment. The DNase I dimer generally appears as a compact globular structure after binding to dsDNA. During sliding or digestion along the DNA backbone, a transient two-lobed morphology (cyan arrows) is observed at 27-29 s and 42-46 s (green frames). **(B)** Cross-sectional height-profile comparison of the DNase I dimer at 26 s, 28 s, and 44 s. The similar molecular dimensions before and during the two-lobed frames indicate that the observed morphology is not caused by scan-induced stretching or motion-blur artifacts. **(C)** Calculated molecular volume of the DNase I dimer over time. The molecular volume largely maintained during the two-lobed frames, although small fluctuations occur due to height-threshold-based volume estimation. Together with the cross-sectional height profiles in **(B)**, this analysis supports that the apparent two-lobed morphology reflects the dimeric organization of DNase I rather than an imaging artifact.

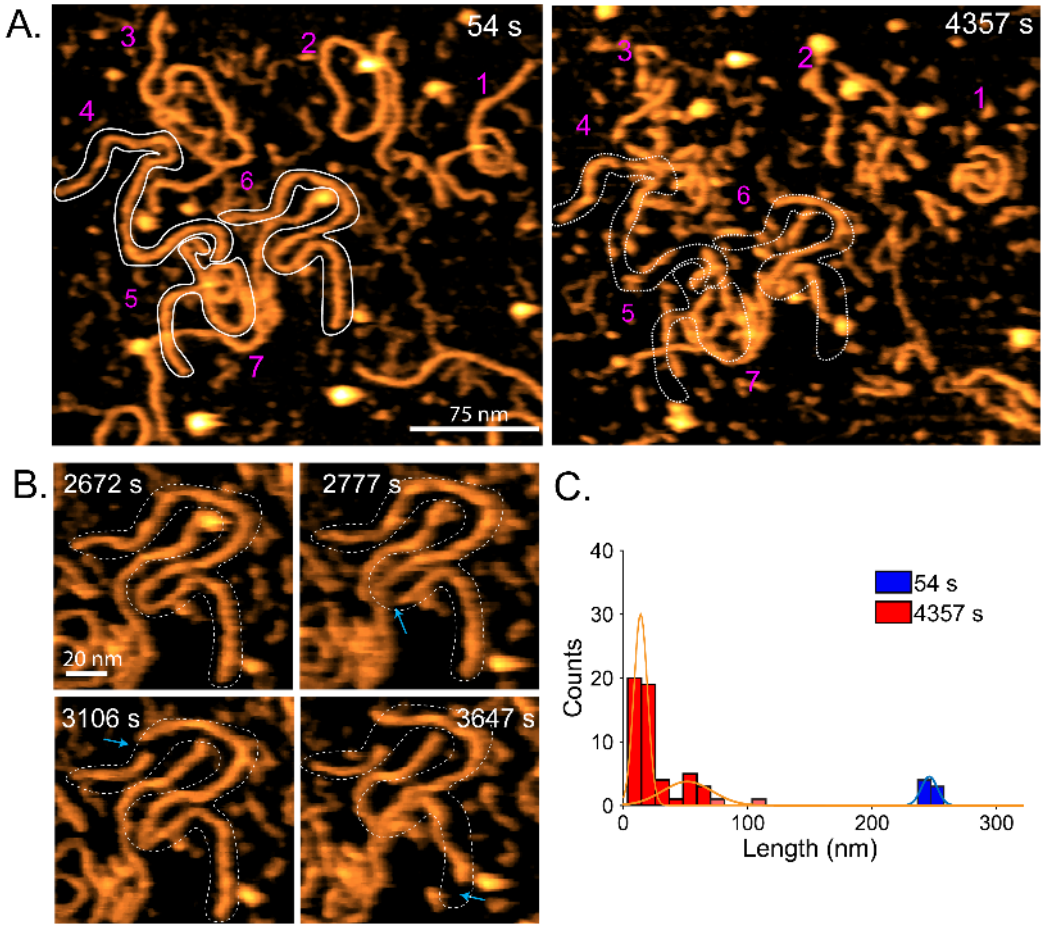


**Figure S9. DNase I cleavage activity on linear 800 bp dsDNA sample. Extended data for Fig 3. (A)** Representative images of seven linear dsDNA molecules before (left, 54 s) and after DNase I digestion (right, 4357s). **(B)** Zoom-in HS-AFM images of DNA molecule 6 with three observed ds-cleavages by DNase I. **(C)** Length histogram of seven monitored dsDNA molecules before and after DNase I digestion. The seven DNA molecules exhibit an average length of 246±7 nm before digestion. At the end of observation, the monitored DNA molecules are cleaved by DNase I into small fragments with two populations, one is shorter than 20 nm and another is within 20-100 nm. The Gaussian fits are summarized in **Table S4**.

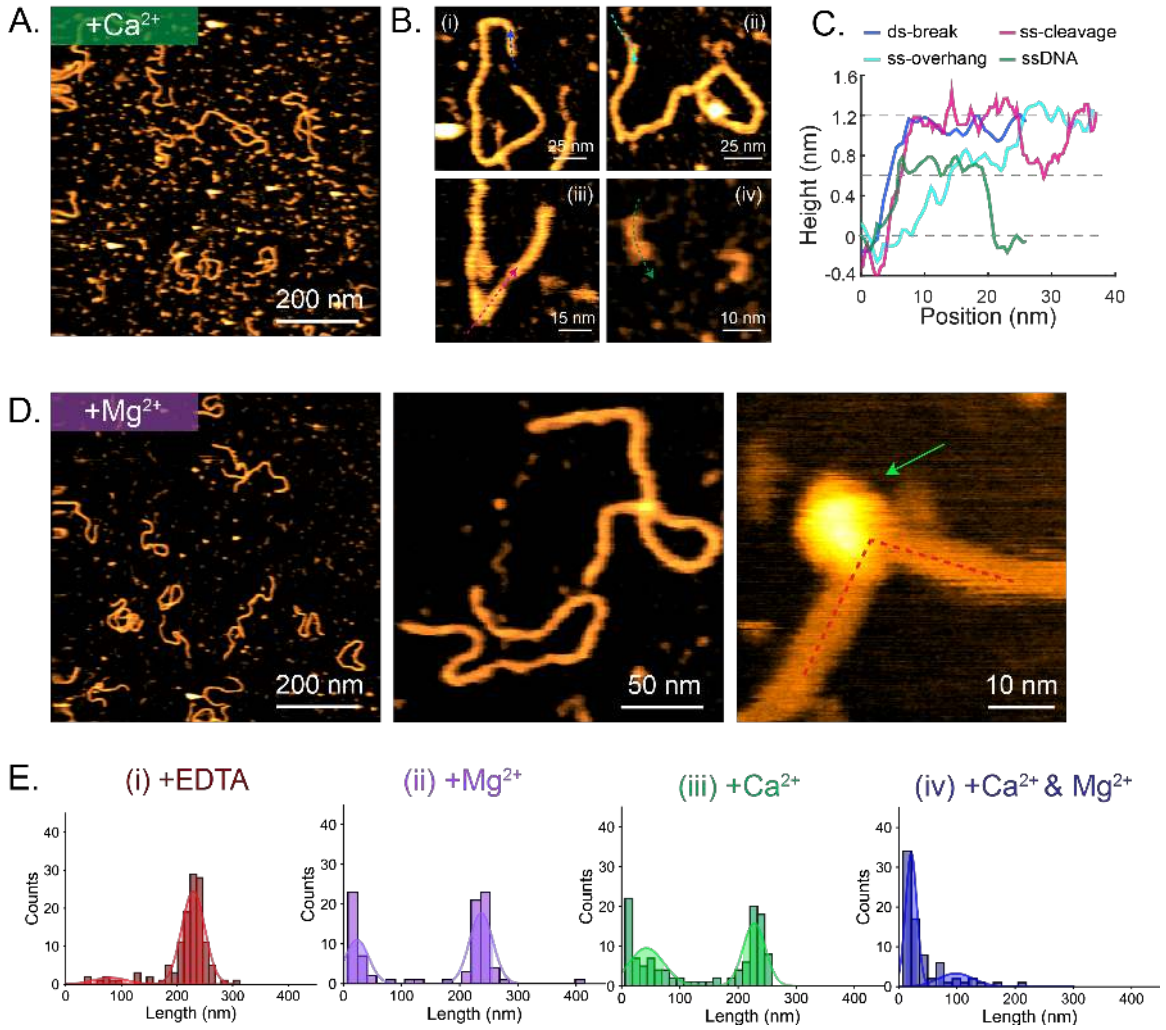


**Figure S10. Effect of divalent cations on DNase I digestion of synthetic 800 bp linear dsDNA. (A-D)** Representative HS-AFM images of DNA fragments degraded by DNase I in buffers **(A-B)** containing $Ca^{2+}$ and **(D)** $Mg^{2+}$ alone, following a 30 min preincubation of DNase I with dsDNA. **(B)** Classification of four distinct cleavage product types observed in the presence of $Ca^{2+}$ alone: (i) DNA fragment produced by ds-breaks, (ii) fragment with a ss-overhang, (iii) partial ss-cleavage along the dsDNA backbone, and (iv) fully ss-DNA fragments. **(C)** Height profiles measured along the backbone of cleavage products, as highlighted by arrows in **(B).** DNase I monomer bends the dsDNA upon binding **(D**, right most panel**)**. **(E)** Length distribution of observed DNA products in four different buffers, highlighting cation-dependent differences in cleavage outcomes. The Gaussian fits are summarized in **Table S4**.

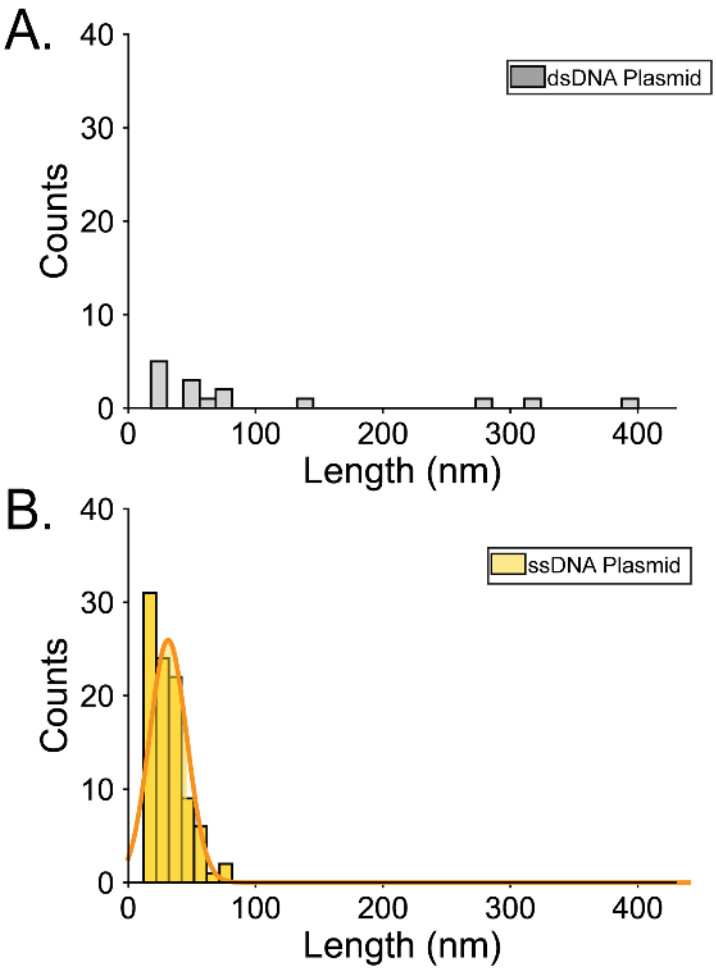


**Figure S11. Effect of divalent cations on DNase I digestion of ssDNA and dsDNA plasmids. Extended data for Figure 5. (A-B)** Length histograms of observed DNA products after 30 min of DNase I digestion of the **(A)** dsDNA plasmid (grey) and **(B)** ssDNA plasmid (yellow) in buffer containing $Mg^{2+}$ and $Ca^{2+}$. The Gaussian fit is summarized in **Table S4**. Consistent with the higher cleavage efficiency of DNase I toward dsDNA, only a small number of relatively long residual DNA products were observed for the dsDNA plasmid in **(A)**.

## Supplementary Tables

**Table S1. Summarized PDB structures of DNase I in Protein Data Bank**

| PDB ID | Technique | Divalent Ions | Macromolecular Ligands |
|---|---|---|---|
| 1DNK | X-Ray diffraction | - | DNA |
| 3DNI | X-Ray diffraction | $Ca^{2+}$ | - |
| 2DNJ | X-Ray diffraction | - | DNA |
| 4AWN | X-Ray diffraction | $Ca^{2+}$, $Mg^{2+}$ | - |
| 3W3D | X-Ray diffraction | $Ca^{2+}$ | G-Actin |
| 2A40 | X-Ray diffraction | $Ca^{2+}$, $Mg^{2+}$ | Actin |
| 1ATN | X-Ray diffraction | $Ca^{2+}$ | Actin |
| 2A41 | X-Ray diffraction | $Ca^{2+}$, $Mg^{2+}$ | Actin |
| 9FJU | Cryo-EM | $Mg^{2+}$ | F-Actin |
| 9FJY | Cryo-EM | $Mg^{2+}$ | F-Actin |
| 2D1K | X-Ray diffraction | $Ca^{2+}$, $Mg^{2+}$ | Actin |
| 7NXV | X-Ray diffraction | $Ca^{2+}$ | Actin |
| 2A3Z | X-Ray diffraction | $Ca^{2+}$, $Mg^{2+}$ | Wiskott-Aldrich syndrome protein, Actin |
| 3CJC | X-Ray diffraction | $Ca^{2+}$ | Actin |
| 7NZM | Cryo-EM | $Mn^{2+}$ | Eukaryotic translation initiation factor 2 subunit 1, Serine/threonine-protein phosphatase PP1-alpha catalytic subunit, Actin |

**Table S2. Summarized HS-AFM imaging buffers used for this study**

| Buffer # | Buffer Composition | Corresponding Figure(s) |
|---|---|---|
| 1 | 10 mM Tris HCl pH 7, 30 mM KCl, 0.1 mM EDTA, | Fig. 1B, Fig. 4A, Fig. 4E, Fig. 5, Fig. S9C, Fig. S10E |
| 2 | 10 mM Tris HCl pH7, 30 mM KCl, 5 mM $MgCl_2$, 0.5 mM $CaCl_2$ | Fig. 1C, Fig. 1F, Fig. 4B-E, Fig. 5, Fig. S1B, Fig. S9C, Fig. S10E, Fig. S11 |
| 3 | 10 mM Tris HCl pH7, 30 mM KCl, 1 mM EDTA | Fig. 1E |
| 4 | 20 mM Tris HCl pH 7, 150 mM KCl, 2.5 mM $MgCl_2$, 0.5 mM $CaCl_2$ | Fig. 2A-D, Fig. S2-S4 |
| 5 | 10 mM Tris HCl pH 7, 150 mM KCl, 2.5 mM $MgCl_2$, 0.5 mM $CaCl_2$ | Fig. 2E-G, Fig. S6-S8 |
| 6 | 10 mM Tris HCl pH 7, 30 mM KCl, 2.5 mM $MgCl_2$, and 0.5 mM $CaCl_2$ | Fig. 3, Fig. S9 |
| 7 | 10 mM Tris HCl pH 7, 30 mM KCl, 0.5 mM $CaCl_2$ | Fig. S10A-C, Fig. S11E |
| 8 | 10 mM Tris HCl pH 7, 30 mM KCl, 5 mM $MgCl_2$ | Fig. S10D-E |
| 9 | 10 mM Tris HCl pH7, 30 mM KCl, 0.66 mM $MnCl_2$, 0.5 mM $CaCl_2$ | Fig. S5 |
| 10 | 10 mM Tris HCl pH 7, 30 mM KCl, 5 mM EDTA | Dilution Buffer |

**Table S3. Gaussian fits of DNase I volume distribution measured in EDTA or $M^{2+}$ conditions.**

| Experiment | Figure | Gaussian Fit | Mean ($nm^3$) | Standard Deviation ($nm^3$) | Probability | Assignment |
|---|---|---|---|---|---|---|
| DNase I in EDTA Buffer (Buffer 1) | Fig. 1B | 1 | 111.3 | 16.2 | 0.52 | Monomer |
| | | 2 | 191.9 | 30.0 (upper limit) | 0.27 | Dimer |
| | | 3 | 320.0 | 30.0 (upper limit) | 0.21 | Trimer |
| DNase I in $M^{2+}$ Buffer (Buffer 2) | Fig. 1C | 1 | 110.0 | 22.6 | 0.54 | Monomer |
| | | 2 | 191.6 | 30.0 (upper limit) | 0.30 | Dimer |
| | | 3 | 325.1 | 30.0 (upper limit) | 0.16 | Trimer |

**Table S4. Gaussian fitting results of DNA degradation products by DNase I under different biochemical conditions.**

| Experimental Conditions | Mixing Strategy[#1] | Figures | Length Distribution Fitting[#2] | | | |
|---|---|---|---|---|---|---|
| | | | Gaussian Fit # | Mean (nm) | Standard Deviation (nm) | Probability |
| Synthetic, linear 800 bp dsDNA. + EDTA (Buffer 1) | In buffer | Fig. 4E, Fig. S10E | 1 | 80.0 | 30.0 | 0.09 |
| | | | 2 | 229.1 | 20.8 | 0.91 |
| Synthetic, linear 800 bp dsDNA + $Ca^{2+}$ (Buffer 7) | In buffer | Fig. S10E | 1 | 42.6 | 30.0 | 0.49 |
| | | | 2 | 229.1 | 19.2 | 0.51 |
| Synthetic, linear 800 bp dsDNA. + $Mg^{2+}$ (Buffer 8) | In buffer | Fig. S10E | 1 | 23.5 | 20.0 | 0.38 |
| | | | 2 | 236.8 | 20.0 | 0.62 |
| Synthetic, linear 800 bp dsDNA. +$Ca^{2+}$/$Mg^{2+}$ (Buffer 2) | In buffer | Fig. 4E, Fig. S10E | 1 | 21.5 | 9.8 | 0.77 |
| | | | 2 | 98.2 | 30.0 | 0.23 |
| Synthetic, linear 800 bp dsDNA. no DNase I (Buffer 6) | Live addition to liquid cell | Fig. S9C | 1 | 246.0 | 7.0 | - |
| Synthetic, linear 800 bp dsDNA. + DNase I (Buffer 6) | Live addition to liquid cell | Fig. S9C | 1 | 14.0 | 5.5 | 0.69 |
| | | | 2 | 51.4 | 20.0 | 0.31 |
| Circular ss-plasmid. + $Ca^{2+}$/$Mg^{2+}$ (Buffer 2) | In buffer | Fig. S11 | 1 | 31.3 | 14.5 | 1 |
| Circular ds-plasmid. + $Ca^{2+}$/$Mg^{2+}$ (Buffer 2) | In buffer | Fig. S11 | n=15, not enough data for statistical analysis | | | |

[#1] Reaction strategy indicates whether DNase I and DNA were mixed on mica, added during live imaging, or preincubated in solution before product deposition onto mica for HS-AFM imaging.
[#2] The length analysis was threshold the analyzed particles need to be longer than 6.0 nm.

**Supplementary Video Captions**

**Supplementary Movie 1.** Representative HS-AFM movie of monomeric DNase I in ETDA with increased structural flexibility **(Figure 1D)**. Scale bar: 5 nm. Imaging parameters: 2 frame/s, 0.25 nm/pixel.

**Supplementary Movie 2.** Representative HS-AFM movie of monomeric DNase I in the presence of $Mg^{2+}$ and $Ca^{2+}$ **(Figure 1E)**. Scale bar: 5 nm. Imaging parameters: 1 frame/s, 0.25 nm/pixel.

**Supplementary Movie 3.** HS-AFM movie of the realtime cleavage of linear 800 bp dsDNA sample, purified from a HPV-16 plasmid, by DNase I aggregates (likely a trimer) in the presence of $Mg^{2+}$ and $Ca^{2+}$ (**Figure 2A-2D**). White arrows indicate DSBs while purple arrows indicate SSBs. Scale bar: 100 nm. Imaging parameters: 1 frame/s, 0.81 nm/pixel.

**Supplementary Movie 4.** Representative HS-AFM movie of real time cleavage of a synthetic, linear, 800 bp dsDNA sample by DNase I monomers (red circle) and a DNase I dimer (green circle) in $Mn^{2+}$ (**Figure S5A**). Cyan arrows indicate site of DSB. Scale bar: 50 nm. Imaging parameters: 1 frame/s, 0.5 nm/pixel.

**Supplementary Movie 5.** HS-AFM movie of the realtime cleavage of synthetic 800 bp linear dsDNA sample by a DNase I dimer in the presence of $Mg^{2+}$ and $Ca^{2+}$ (**Figure 2E**). Scale bar: 20 nm. Imaging parameters: 1 frame/s, 0.33 nm/pixel.

**Supplementary Movie 6.** Representative HS-AFM movie of realtime digestion of original dsDNA#4 by DNase I molecules (**Figure 3B**). Scale bar: 20 nm. Imaging parameters: 1 frame/s, 0.25 nm/pixel.

**Supplementary Movie 7.** Representative HS-AFM movie of DNase I interacting with synthetic 800 bp linear dsDNA in EDTA (**Figure 4A**). Due to the lack of the divalent cations, the observed DNase I molecules are unable to cleave dsDNA. Scale bar: 100 nm. Imaging parameters: 1 frame/s, 0.5 nm/pixel.